SCALING OF PARAMETERS AND RESONANCE SELF-ABSORPTION IN CO LASERS

W. B. Lacina, et al

Northrop Research and Technology Center

Prepared for:

Office of Naval Research
Advanced Research Projects Agency

September 1974

UNCLASSIFIED

SECURITY CLASSIFICATION OF THIS PAGE (When Data Entered)

REPORT DOCUMENTATION PAGE		READ INSTRUCTIONS BEFORE COMPLETING FORM
1. REPORT NUMBER NRTC 74-48R	2. GOVT ACCESSION NO.	3. RECIPIENT'S CATALOG NUMBER AD/A-002209
4. TITLE (and Subtitle) Scaling of Parameters and Resonance Self-Absorption in CO Lasers (U)		5. TYPE OF REPORT & PERIOD COVERED Technical Report 6. PERFORMING ORG. REPORT NUMBER
7. AUTHOR(s) W. B. Lacina, G. L. McAllister		8. CONTRACT OR GRANT NUMBER(s) N00014-72-C-0043
9. PERFORMING ORGANIZATION NAME AND ADDRESS Northrop Research and Technology Center 3401 West Broadway Hawthorne, California 90250		10. PROGRAM ELEMENT, PROJECT, TASK AREA & WORK UNIT NUMBERS ARPA Order No. 1806
11. CONTROLLING OFFICE NAME AND ADDRESS Advanced Research Projects Agency 1400 Wilson Blvd, Arlington, VA 22209		12. REPORT DATE September 1974 13. NUMBER OF PAGES 30
14. MONITORING AGENCY NAME & ADDRESS(if different from Controlling Office) Office of Naval Research Department of the Navy Arlington, Virginia 22217		15. SECURITY CLASS. (of this report) UNCLASSIFIED 15a. DECLASSIFICATION DOWNGRADING SCHEDULE

16. DISTRIBUTION STATEMENT (of this Report)

None.

17. DISTRIBUTION STATEMENT (of the abstract entered in Block 20, if different from Report)

None.

18. SUPPLEMENTARY NOTES

None.

19. KEY WORDS (Continue on reverse side if necessary and identify by block number)

CO Laser
Electric Discharge
Scaling Generalizations

20. ABSTRACT (Continue on reverse side if necessary and identify by block number)

High optical extraction efficiencies for CO electric discharge lasers have been theoretically predicted and experimentally demonstrated. Considerable interest for military applications has resulted in programs for development of both pulsed and cw CO EDL's with high power and high energy objectives. In order to make realistic performance predictions for potential device design, it is necessary to understand how these devices scale in volume, pressure, and other parameters. In this report, several generalizations that result

DD FORM 1 JAN 73 1473 EDITION OF 1 NOV 65 IS OBSOLETE

UNCLASSIFIED

SECURITY CLASSIFICATION OF THIS PAGE (When Data Entered)

from parametric scaling of the CO laser kinetics will be reported and compared with experimental data from an e^--beam stabilized device. Scaling to high energy and high power systems will be discussed. The limitations on high pressure or line-selected operation that may be imposed by resonant self-absorption in the CO medium will be discussed. Preliminary investigations suggest that this effect may be an important pressure-dependent mechanism, with possible consequences for attainment of line selection objectives. It will also be shown that certain presently unexplained discrepancies (relating to transient time scale, spectral anomalies, efficiency degradation, and sensitive temperature dependence) might all be consistently resolved by this mechanism.

NRTC 74-48R

SCALING OF PARAMETERS AND RESONANCE SELF-ABSORPTION IN CO LASERS

September 1974

Prepared by

W. B. Lacina and G. L. McAllister

Contract No. N00014-72-C-0043

Sponsored by

ADVANCED RESEARCH PROJECTS AGENCY
ARPA ORDER No. 1806

Monitored by
OFFICE OF NAVAL RESEARCH
CODE 421

Northrop Research and Technology Center
High Power Laser Program Office
3401 West Broadway
Hawthorne, California 90250

Telephone: (213) 675-4611, Ext. 2821

NOTICE

The views and conclusions contained in this document are those of the author and should not be interpreted as necessarily representing the official policies, either expressed or implied, of the Advanced Research Projects Agency or the U. S. Government.

TABLE OF CONTENTS

HIGH ENERGY SCALING GENERALIZATIONS FOR CO ELECTRIC DISCHARGE LASERS (U)

W. B. Lacina and G. L. McAllister
Northrop Research and Technology Center
Hawthorne, California

ABSTRACT
(Unclassified)

High optical extraction efficiencies for CO electric discharge lasers have been theoretically predicted and experimentally demonstrated. Considerable interest for military applications has resulted in programs for development of both pulsed and cw CO EDL's with high power and high energy objectives. In order to make realistic performance predictions for potential device design, it is necessary to understand how these devices scale in volume, pressure, and other parameters. In this paper, several generalizations that result from parametric scaling of the CO laser kinetics will be reported and compared with experimental data from an e⁻-beam stabilized device. Scaling to high energy and high power systems will be discussed. The limitations on high pressure or line-selected operation that may be imposed by resonant self-absorption in the CO medium will be discussed. Preliminary investigations suggest that this effect may be an important pressure-dependent mechanism, with possible consequences for attainment of line selection objectives. It will also be shown that certain presently unexplained discrepancies (relating to transient time scale, spectral anomalies, efficiency degradation, and sensitive temperature dependence) might all be consistently resolved by this mechanism.

1. INTRODUCTION

(U) Because of its favorable operating characteristics of high quantum efficiency and high specific output power, the CO electric discharge laser has attracted considerable interest as a candidate for both pulsed and supersonic cw devices. Electron beam-stabilized CO EDL's have been shown to operate[1] at efficiencies >65% with specific energies >750J/ℓ/atm, and high output energies (>1200 J) have been demonstrated[2] with a 20 liter pulsed device. Five hundred joules (500 J) with 40% efficiency has recently been obtained at our laboratory from a device with 7 liters active volume, using a $CO/N_2/Ar = 1/9/7$ mixture of 190 Torr at 80°K. Development of supersonic flow cw devices is currently in progress at several laboratories, and results that have been obtained at Mathematical Sciences Northwest and Northrop will be reported in a separate presentation[3] of this Conference.

(U) Development of these devices for high power, high energy military applications requires that a number of coupled technological and fundamental physical questions be addressed. The optimistic theoretical predictions are based on laser kinetic models that make several important assumptions, many of which are necessarily approximations, while others may be omissions. In general, results of calculations have agreed reasonably well with experimental comparisons, although there remain some discrepancies which need to be definitively resolved in order that realistic predictions and device design can be made with confidence. In order to achieve military objectives of HIGH ENERGY pulsed or HIGH POWER cw devices, the laws for scaling in volume and pressure must be correctly understood. In addition, for some applications for which line selection of only those transitions with high atmospheric transmission is required, the consequences of scaling laser parameters subject to spectral constraints must also be assessed. Scaling in volume for these devices presents problems primarily only from component limitations, while scaling in pumping and pressure correspond to the basic physical mechanisms of the CO laser, which are described by the molecular and electron kinetics processes and the interaction of the gain medium and the optical extraction.

(U) In this paper, several scaling generalizations for a (pulsed or cw) high pressure CO EDL are presented and compared with experimental data from a pulsed, e^--beam stabilized device. The scaling of parameters necessary for analysis of specific problems in terms of more general results is discussed, and it is shown that the transient evolution of the system is mainly dependent only upon the total energy deposition into CO as a function of time. However, the validity of these parametric scaling laws is based on a model which may be inadequate to correctly describe effects of high pressure (≥100 Torr) operation, because of the possibility that resonant self-absorption may be an important effect. All contemporary theoretical models of CO laser kinetics have overlooked the fact that laser oscillation on one line could be absorbed by near-resonant transitions of other bands. This possibility is currently under investigation, and completely self-consistent calculations accounting for this phenomenon will be completed shortly and reported in the near future. After presenting a summary of the results of scaling the laser kinetics without inclusion of these effects, a discussion of several important consequences that resonant self-absorption may present for high pressure devices will follow. It will also be shown that certain presently unexplained discrepancies (relating to transient time scale, spectral anomalies, efficiency degradation, and temperature dependence) might all be consistently resolved by this mechanism. It will be necessary to understand the possible implications of this effect and the limitations that it may impose in order to determine and optimize design considerations for high pressure and line-selected devices.

2. THEORETICAL MODEL

(U) A molecular kinetic model for an electrically excited (CO, N_2, Ar, He, ...) gas mixture has been constructed for the calculation of the radiative characteristics of a CO laser oscillator or amplifier. A computer program for the numerical solution of the steady state or transient

master equation for the diatomic species has been developed to predict vibrational population distributions, gain and saturation parameters, energy transfer and extraction rates, conversion efficiencies, output intensities, and spectral distributions. The radiative calculations are self-consistent with the saturated gain on all oscillating transitions equal to the losses. The plasma characteristics, described by a Boltzmann distribution, are adjusted self-consistently in the calculation as a function of time to account for electron heating for a given temporal input power. A more complete discussion of the assumptions upon which this model is based has been given elsewhere,[4,5] where numerical results for a variety of operating conditions were presented and compared with experimental data from a pulsed high pressure e^--beam stabilized electric discharge CO laser oscillator. Similar analytical work on the CO EDL has been presented by numerous others.[6-10]

(U) It is possible to make several reasonable approximations that allow certain general scaling laws for a CO EDL to be formulated.[11] These generalizations depend only upon a few basic parameters which make it possible to predict the temporal output characteristics of a large class of both pulsed and flowing cw CO systems. Although the present theoretical results are limited to gas mixtures containing CO and monatomic diluents only, comparisons with experimental data for both CO/Ar and CO/N_2 are included. It is found experimentally that the excitation times required to attain threshold and steady state agree with the scaling results predicted for CO/Ar. Uncertainties in the CO-N_2 and N_2-N_2 VV rates make theoretical analysis for CO/N_2 mixtures less reliable. However, the experimental results indicate that CO/N_2 systems can be scaled similarly.

(U) Thus, good qualitative interpretation of both CO/Ar and CO/N_2 data can be made. It can be concluded from these results that a general CO/X system containing either monatomic or N_2 diluents can be characterized by the temporal energy deposition into the CO vibrational states. Thus, except for the spectral details, it is possible to design general CO/X systems to a very good approximation without resorting to extensive computer calculations.

(U) The physics of the present theoretical model is described by four basic systems of equations that couple the CO vibrational state population densities, the radiation intensities, the gas kinetic temperature, and the plasma kinetic parameters (electron density and temperature) as a function of time. Since the general formulation of these equations and the assumptions made have been described previously,[5] they will be summarized only briefly here. Certain approximations (most of which are not required for the complete computer analysis) make it possible to obtain a variety of general results in terms of a very small set of scale parameters.[11] In fact, one basic parameter related to pumping is all that is required to present a reasonably simple description of the CO EDL under the set of approximations to be discussed below.

(U) The physics of the molecular kinetic processes is described by the master equation for vibrational population densities n_v of the CO molecule,

$$dn_v/dt = R_v^e + \sum_X R_v^{VT}(CO, X) + R_v^{VVT}(CO, CO)$$

$$+ R_v^{VVT}(CO, N_2) + R_v^{spon} + R_v^{stim} \qquad (1)$$

with pumping and relaxation processes which include: (1) electron impact excitation of the vibrational states, (2) vibration to translation (VT) deactivation processes, (3) near resonant vibration to vibration (VVT) single quantum exchange collisions, (4) spontaneous radiative decay, and (5) stimulated emission and absorption processes. Sources for rates have been summarized previsouly.[5]

(U) Radiation intensities are calculated by requiring that the gain coefficients for all oscillating transitions be equal to the loss coefficient at all times. The rotational levels are assumed to be in thermal equilibrium with the molecular kinetic temperature, and rotational cross-relaxation is assumed to be sufficiently fast that only one rotational line can oscillate in any given vibrational band. Losses such as mirror absorption, output coupling, window losses, or intracavity line selection losses are all assumed to be uniformly distributed throughout the laser gain medium. These cavity losses are assumed to be small enough that the approximation of a spatially uniform intensity distribution over the length of the active medium is adequate for describing the molecular and radiative characteristics of the medium. The optical resonator is assumed to be formed by two plane parallel mirrors (one totally reflecting, the other with reflectivity R) separated by a distance L. From the oscillator gain conditions, $R\exp[2(\alpha-\beta)L] = 1$, the gain coefficient α for an oscillating line (for $R \sim 1$) must be equal to the threshold loss $\gamma = \beta + (1 - R)/2L$, where β is the loss coefficient for the cavity exclusive of the output coupling.

(U) The analysis assumes that the plasma kinetics can be treated with a Boltzmann electron distribution, with a self-consistent adjustment of the electron density and effective temperature as a function of time to produce a prescribed temporal input excitation power characterized by a rise and fall time. Physically, the choice of that form for the electrical excitation power is appropriate for an e^--beam sustained CO device with the rise time related to the approach to steady state of the electron density and the fall time to the decay of the sustainer voltage due to the discharge of a capacitor bank.

(U) Gas heating from VV and VT kinetic processes, as well as from rotational equilibration accompanying stimulated emission results in a temporal rise in the molecular temperature. The effects of temperature rise are included in the analysis.

(U) In order to derive a useful set of generalized results that can easily be scaled, it is first necessary to simplify the equations by introducing approximations that will reduce the number of scale parameters required to a reasonable minimum value. Although the additional

approximations to be discussed here are neither required nor invoked in the complete computer analysis, they will be useful for summarizing the results of the computer calculations in a coherent way. The objective here is to show that a rather general class of pulsed CO oscillators can be described quite accurately in terms of only two basic scale parameters that define the electrical pumping and cavity threshold.

(U) For a high pressure oscillator operating at temperatures typically in the range 60-300°K, the spontaneous radiation and VT decay terms in the master equation can be neglected. Consistent with this approximation, the VT contribution to the kinetic heating can also be neglected. It will be convenient to refer to the initial values of the temperature T_{mol} and pressures p_{CO}, p_X in the results of calculations to be presented here. Theoretical prediction that only a small percentage of electrical power is converted to kinetic heating (typically ~10-20%), even after steady state has been attained, have been experimentally verified.[12] Thus, for reasonably dilute CO gas mixtures, it is a good approximation to neglect the temperature rise for pulse times that are comparable to the time required to reach steady state. Although the calculations correspond to fixed number densities, the pressures will change by only a small fraction during that time scale. All of the calculations to be presented here correspond to cases for which the electrical excitation was kept constant as a function of time during the pulse, with temporal evoltuion of the electron temperature T_e.

(U) The coupled set of equations of reference (5) with the approximation discussed above can be written in dimensionless form by introducing the following quantities:

$$
\begin{aligned}
x_v &= n_v/N_{CO} \\
x_e &= n_e/N_{CO} \\
\tau &= p_{CO}t \\
f &= 1 + (3/2)p_{tot}/p_{CO} \\
\xi &= \Delta\nu_{CO}/\Delta\nu_{tot} \\
&= \frac{p_{CO}\langle v_{rel}(CO, CO)\rangle\sigma^{opt}(CO, CO)}{\sum_X p_X\langle v_{rel}(CO, X)\rangle\sigma^{opt}(CO, X)} \qquad (2) \\
\tilde{\gamma} &= \gamma/\xi \\
\tilde{W}_e &= W_e/p_{CO}^2 \\
\tilde{I} &= I\xi/p_{CO}^2 \\
\tilde{E} &= E/p_{CO}
\end{aligned}
$$

where x_v are the relative populations, x_e is a measure of the degree of ionization, f is related to the number of thermal degrees of freedom, and ξ is the fractional percentage of total optical

line broadening caused by CO. $\tilde{\gamma}$, $\tilde{W}$, $\tilde{I}$, and $\tilde{E}$ are scaled threshold loss (cm^{-1}), power density [$W/cm^3/Torr\ (CO)$], intensity [$W/cm^2/Torr^2(CO)$], and energy density [$J/cm^3/Torr(CO)$]. The definition of the parameter ξ given here applies to a situation in which pressures are high enough ($\geq$20 Torr) that optical lines are predominantly pressure broadened.

(U) If these scale parameters are introduced, the master equation expresses the evolution of the relative populations x_v as a function of scale time $\tau = p_{CO}t$. This is to be expected, since the electrical excitation is kept constant, and the dominant kinetic processes are (two body) VV collisions. Thus, the physics of the molecular vibration states depends explicitly only upon the kinetic temperature and the scaled electrical excitation $\tilde{W}_e = W_e/p_{CO}^2$. Implicitly, however, it depends also upon the scaled threshold loss coefficient $\tilde{\gamma}$ for the cavity due to the oscillation condition, and upon the parameter f due to the kinetic heating.

(U) It is apparent that the set of parameters (T_{mol}, $\tilde{W}_e$, $\tilde{\gamma}$, f) completely characterize the CO EDL under these approximations; all other inputs to the mathematical model consist only of fundamental physical constants. In the following section, a variety of numerical results based on the complete computer analysis for this model will be presented and discussed to show the relative sensitivity of these parameters.

3. THEORETICAL RESULTS

(U) Computer calculations were carried out for a fixed value f = 16 (corresponding to a dilute, 10% CO mixture). The kinetic temperatures T_{mol} included (60, 100, 150, 200, 300)°K, the scaled electrical pumping rates (0.2, 0.5, 1.0, 2.0, 5.0, 10, 20, 50, 100, 200)$W/cm^3/Torr^2$, and the scaled threshold loss coefficients (0.1, 0.2, 0.5, 1.0, 3.0, 7.0, 10, 20)%/cm. From the results of any given case specified completely by the set of four parameters (T_{mol}, $\tilde{W}_e$, $\tilde{\gamma}$, f), the general class of problems that can be scaled exactly from those results is quite restrictive; it allows only the variation of the CO partial pressure, provided that the electrical excitation W_e is scaled by p_{CO}^2, and that the threshold level and gas mixture ratio are held constant. However, except for the scaled excitation power $\tilde{W}_e$, most of these parameters do not have a sensitive effect on the power response of the system as a function of time (although detailed spectral predictions may have a more critical dependence). Thus, the class of problems that can be analyzed from a given case is often more extensive than that just described. The reasons for this are the following: (1) the most important parameter, the scaled excitation $\tilde{W}_e$, is a measure of the electrical pumping per molecule relative to the rate of VV cross-relaxation, and thus specifies the ratio of the two dominant kinetic processes in the CO EDL. (2) A pulsed high pressure CO EDL typically operates in a regime where oscillation is high above threshold, and thus, results for optical power extraction will usually be insensitive to the scaled cavity loss coefficient $\tilde{\gamma}$. Unless the ratio $\tilde{W}_e/\tilde{\gamma}$ becomes very small the medium intensity will be high above the saturation intensity, and the optical output will be independent of $\tilde{\gamma}$. (3) The temperature rise for pulse times comparable to the time required to reach steady state is small, so the results do not depend critically upon f, providing it is large. This parameter is mainly

important for detailed predictions of spectral distribution. (4) Results of calculations for systems operating with parameters in the above ranges do not show a significant sensitivity to dependence on T_{mol}.

(U) Figure 1 shows plots of the quantum power efficiency (for the total optical conversion of electrical input) for a variety of different values of $\tilde{W}_e$ as a function of $p_{CO}t$, for $T_{mol} = 100^{\circ}K$. Results of calculations show that the most important parameter for small values of $\tilde{Y}$ is the scaled excitation power $\tilde{W}_e$, and that the optical output is relatively insensitive to $\tilde{Y}$ for small values of $\tilde{Y}$. It is apparent from Figure 1 (and from similar results for other values of $\tilde{Y}$ and T_{mol}) that the optical output efficiency displays a remarkably similar behavior over a wide range of the parameter $\tilde{W}_e$. In fact, these results can be used to show that, for a given temperature T_{mol} and a fixed value of quantum efficiency η/η_∞ (where η_∞ is the steady state value), a loglog plot of $p_{CO}t$ versus the scaled power $\tilde{W}_e$ is approximately linear. For example, Figure 2 shows such a plot for the turn-on time $p_{CO}t_o$ (obtained by extrapolating the curves of Figure 1 to the origin and neglecting a small initial bump that often occurs in the calculations) versus $\tilde{W}_e$. The slope of these curves is approximately -5/6 and is independent of T_{mol} and $\tilde{Y}$; the variation in the magnitude of the curves is less than a factor of two within the range of temperatures chosen. The turn-on time corresponds to the point where $\eta = 0$; however, it is apparent that the curves of Figure 1 remain similar as time evolves. Thus, for a fixed temperature T_{mol}, the time t required to attain any specified value η/η_∞ for the optical extraction efficiency satisfies

$$\tilde{e} = p_{CO}t\,\tilde{W}_e^{5/6} = \text{constant}, \qquad (3)$$

which implies that, within a range of values for $\tilde{Y}$ which are suitably small, a "universal" plot of efficiency versus the parameter $\tilde{e} = p_{CO}t\tilde{W}_e^{5/6}$ can be constructed. As an example, all of the plots for the conditions of Figure 1 can be summarized as shown in Figure 3. (The value of the steady state efficiency η_∞ depends only slightly upon $\tilde{W}_e$, T_{mol} and $\tilde{Y}$.) The significance of the parameter $\tilde{e}$ can be seen by noting that if the exponent of $\tilde{W}_e$ in Eq. (3) were unity instead of 5/6, $\tilde{e}$ would represent the total electrical energy $\tilde{E} = W_e t/p_{CO}$ [J/ℓ/Torr(CO)] which has been deposited into CO vibrational energy up to time t. Therefore, the response of the system is approximately a function only of the specific input energy $\tilde{E}$ (which is, of course, a function of time and the excitation rate). The power efficiency can be integrated to give a universal curve for the energy efficiency ϵ/η_∞ as a function of the parameter $\tilde{e}$, and this result is also presented in Figure 3.

(U) Among the important conclusions to be drawn from the above remarks are the following. Characteristic times, such as turn-on time or time required to reach steady state, satisfy a relation given by Eq. (3). For the range of temperatures and for the reasonably small values of $\tilde{Y}$ discussed here, turn-on occurs after a specific electrical energy $E_o \sim 0.5 - 1.0$ J/ℓ/Torr (CO has been deposited, and steady state is attained after an energy $E_{ss} \sim 1.7 - 2.6$ J/ℓ/Torr (CO has been deposited. (These numbers correspond to a specific pumping rate $\tilde{W}_e = 1.0$ W/cm^3/Torr

$(CO)^2$; for other values of $\tilde{W}_e$, Eq. (3) shows that these deposition energies increase as $\tilde{W}_e^{1/6}$). The typical range of values for $\tilde{W}_e$ in the data to be presented later is sufficiently small that $\tilde{W}_e^{1/6}$ variation is not significant, and thus, experimental results will be plotted in terms of the more physically significant quantity $\tilde{E} = W_e t/p_{CO}$.

(U) It is interesting to characterize the CO medium by a saturation intensity. Although the full kinetic model contains simultaneous oscillation on several lines, it is convenient to neglect this feature for the moment, and to investigate how the gain saturates as a function of the total intensity in the medium. From the analysis of a simple two-level model, it can be shown that the saturation gain $\alpha(I)$ satisfies

$$\alpha(I) = \alpha_o (1 + I/I_s)^{-1} , \tag{4}$$

where the saturation intensity I_s is independent of the electrical pumping. We shall show that, at steady state, the CO EDL follows a simple dependence of this form, and an estimate of the scaled saturation intensity as a function of T_{mol} will be derived. In terms of scaled quantities, Eq. (4) becomes, upon setting $\alpha(I) = \Upsilon$,

$$\tilde{\Upsilon} + \eta_\infty \tilde{W}_e/\tilde{I}_s = \tilde{\alpha}_o , \tag{5}$$

where the steady state condition $\tilde{\Upsilon}\tilde{I} = \eta_\infty \tilde{W}_e$ has been used. Thus, for a fixed value $\tilde{W}_e$, the steady state oscillator power efficiency η_∞ and the cavity threshold Υ are linearly related if the laser gain medium saturates according to the relation of Eq. (4). That is, if $\eta_\infty(0)$ is the limiting value of the steady state efficiency for $\tilde{\Upsilon} \to 0$ (lossless cavity), then

$$\tilde{\Upsilon} = -[\eta_\infty - \eta_\infty(0)]\tilde{W}_e/\tilde{I}_s \tag{6}$$

(U) Figure 4 shows η_∞ plotted versus $\tilde{\Upsilon}$ for $T_{mol} = 100^oK$, for two different values of $\tilde{W}_e$, and as Eq. (6) shows, the slope $|d\tilde{\Upsilon}/d\eta_\infty|$ of these curves is proportional to $\tilde{W}_e$. Furthermore, the proportionality constant determines the scaled saturation intensity, which is determined from Figure 4 to be $\tilde{I}_s \sim 0.8\ W/cm^2/Torr^2$. Similar plots for a fixed value of $\tilde{W}_e$ and variable temperature T_{mol} are shown in Figure 5. All of these curves are linear to a very good approximation, and the saturation intensities obtained from their slopes are summarized in Table I. During the transient evolution, the relation between the quantum efficiency and the cavity threshold does not seem to follow a linear relationship.

TABLE I. SCALED SATURATION INTENSITY (U)
(Unclassified)

$T_{mol}(^oK)$	60	100	150	200	300
$\tilde{I}_s(W/cm^2/Torr^2)$	0.6	0.8	1.6	2.5	6.4

Small signal gain characteristics can be obtained from Eq. (5) with $\tilde{Y} = 0$. For values of pumping and cavity threshold considered here, it is apparent that the small signal gain is proportional to $\tilde{W}_e$.

$$\tilde{\alpha}_o = \eta_\infty(0)\, \tilde{W}_e/\tilde{I}_s \tag{7}$$

For efficient operation of the oscillator (high above threshold), the necessary condition is $\tilde{\alpha}_o \gg \tilde{Y}$, and therefore (since $\eta_\infty \sim 1$),

$$\tilde{W}_e/\tilde{Y} \gg \tilde{I}_s. \tag{8}$$

4. EXPERIMENTAL COMPARISONS AND CONCLUSIONS

(U) The electrical excitation times required to reach laser threshold and steady state have been measured for CO/Ar and CO/N_2 gas mixtures and are compared below to the scaling generalizations described in Section 3. The laser used for these measurements was an e^--beam stabilized, electric discharge CO laser with a 10 cm x 10 cm x 100 cm discharge region. The operating temperature was 80^oK with gas pressures typically in the range from 50 - 200 Torr. The nominal operating parameters were $E/N = 1.1 \times 10^{-16}$ V cm^2, sustainer current density $I_s = 2 A/cm^2$, and e^--beam current density $I_b = 25$ mA/cm^2. Output energies exceeding 500J/pulse have been obtained. The electrical excitation pulse length was 75 μs and the optical pulse length varied between 20 - 100 μs depending on the electrical excitation rate and the gas mixture used.

(U) The laser output energy was measured with a ballistic thermopile calorimeter (Hadron Series 117) and the temporal pulse shape was monitored with a Ge:Au detector. Figure 6 illustrates a typical pulse shape for CO/N_2 with a nearly constant electrical excitation rate for 75 μs. In this example laser threshold is reached 38 μs after the electrical excitation is initiated and the output lasts considerably longer than the excitation pulse length. This long decay is typical of CO/N_2 gas mixes due to the time required for energy stored in the vibrational levels of nitrogen to be transferred back to the CO molecules. The pulse shapes for CO/Ar mixtures look similar except that the pulse decay time is shorter, since no energy is stored in the argon.

(U) The laser threshold time t_o is taken to be that time from initiation of the sustainer current to the point where the laser intensity of 3 - 5% of the maximum intensity as indicated by the arrow in Figure 6. This threshold is generally sharp and the time is therefore well defined. The steady state time t_{ss} is defined as that time required to reach ~95% of the maximum value, also indicated by an arrow in Figure 6. This value is not as sharply defined as t_o and considerable spread in the data may occur due to the interpretation of when steady state occurs.

(U) It was shown in Section 3 that the inverse of the threshold and steady state times for CO/Ar laser gas mixtures should scale as $p_{CO}\, \tilde{W}_e^{5/6}$, where $\tilde{W}_e$ is the electrical excitation rate

$[W/cm^3/Torr^2(CO)]$. For the range of variables considered, the exponent (5/6) can be taken to be unity with the resulting physical interpretation that, regardless of the excitation rate, fixed specific energies [J/ℓ/Torr(CO)] must be deposited to attain threshold and steady state. Experimental values of threshold and steady state times were measured for CO/Ar gas mixtures from 75 to 150 Torr. The inverse times are plotted in Figure 7 and, as predicted by the scaling generalizations, are proportional to W_e/p_{CO}. From Figure 7 it is concluded that approximately 0.9 J/ℓ/Torr (CO) must be deposited in order to reach threshold, which is in good agreement with the scaling generalizations, which predict that 0.5 - 1.0 J/ℓ/Torr (CO is necessary. The experimental value for the deposited energy required to attain steady state, ~2.0 J/ℓ/Torr (CO), is also in good agreement with the scaling predictions of 1.7 - 2.6 J/ℓ/Torr (CO).

(U) The calculations discussed in Section 3 are valid only for gas mixtures of CO and monatomic diluents. However, the scaling generalizations appear to be valid for CO/diatomic systems, provided that only the fractional energy into the CO system is used for scaling. Experimental measurements of the threshold and steady state times for a fixed CO/N_2 (1:6) mixture are shown in Figure 8. It is apparent from this graph that the inverses of these times scale with W_e just as they do for CO/Ar mixtures although the required total energy deposited is different. This is to be expected because the deposited energy is split between the CO and N_2. It would seem, in fact, that the required energy deposited in the CO vibrational system should be the same regardless of the diluent and that the fractional amount deposited into nitrogen can be determined from the experimental data. That is, a specific energy $E(CO)/p_{CO}$ must be deposited into vibrational excitation of CO in order to attain any given efficiency.

(U) Additional evidence is provided for the previous supposition by measurements of the threshold time dependence on the fractional content of CO, $f_{CO} = p_{CO}/p_{tot}$. This data, shown in Figure 9, indicates that the total specific energy required to achieve threshold increases linearly with f_{CO} which, when extrapolated to $f_{CO} = 1$, gives ~ 0.7J/ℓ/Torr(CO), which agrees approximately with the previous results for CO/Ar mixtures. If it is assumed that the required threshold energy deposited in CO is always 0.7J/ℓ/Torr(CO), the remaining fraction into nitrogen increases linearly with $f_{N_2} = 1 - f_{CO}$, as is also shown in Figure 9. That is,

$$E_o(tot)/p_{tot} = f_{CO} E_o(CO)/p_{CO} + f_{N_2} E_o(N_2)/p_{N_2}. \qquad (8)$$

From the experimental value for $E_o(CO)/p_{CO}$, it is determined that $E_o(N_2)/p_{N_2} = 0.13J/\ell/Torr(N_2)$. The physical interpretation of the experimental data presented in Figure 9 is that the energy deposition per molecule is six times higher than CO than for N_2. Thus, it appears that the scaling generalizations derived for CO/Ar mixtures can also be applied to systems with diatomic diluents, and that accurate knowledge of the large number of kinetic rates required for a complete analysis of the CO/N_2 system is not essential for prediction of approximate laser performance.

5. RESONANT SELF ABSORPTION

(U) An important pressure effect that is not included in the physics of the present kinetic model described in Section 2 is the self-absorption (or enhanced gain) of laser radiation in the medium by coincidental resonances originating from other P and (mostly) R transitions. As the pressure and temperature increase, the collision broadened half-widths of all the CO lines increase, resulting in several significant overlaps for almost every transition. Thus, it is likely that the simple pressure dependence described in the previous sections for scaling the CC laser is probably not completely accurate, and that such a model may be seriously invalid for prediction of detailed spectral distributions. The impact of this phenomenon on previous comparisons between theory and experiment will be described below, and a variety of discrepancies that are currently unexplained will be shown to have a consistent resolution based on the hypothesis of resonant self-absorption. Initial calculations have been carried out using the existing kinetics code for an atmospheric pressure CO EDL at 100°K, pumped at rates typical of present experimental devices (10 kW/cm^3), and these show that self-absorption competes strongly with all other kinetic and excitation rates. A refinement and extension of the laser kinetics computer code has been undertaken to properly include, in a completely self-consistent way, all of the gain and absorption processes to determine radiation intensities for an oscillator. These results will be available shortly, and will be presented in the near future.

(U) The important consequences that are anticipated from this analysis, assuming that the effects are indeed significant, will be described briefly here.

5.1 TRANSIENT TIME SCALE

(U) The absorption of the medium is expected to increase laser threshold time, and probably to lengthen the transient evolution to steady state. Experimental comparisons made previously,[5] as well as those reported above in Section 4, are consistent with this possibility, since experimental times for onset of laser oscillation were always greater than theoretically predicted.

5.2 SPECTRAL ANOMALIES

(U) Theoretical calculations consistently show that predicted output spectral distributions should lie about one or two v-bands lower than what is usually observed. Furthermore, experimental output spectra often show that certain transitions are always missing, and it was from this observation that the hypothesis of resonant self-absorption by accidental coincidences among the CO transitions was first conceived to be an important mechanism. Typically, the resonances result in one of two possible effects: 1) The absorptions are so strong that laser oscillation is permanently inhibited from certain transitions, or 2) oscillation occurs, but output coupling efficiency is degraded and higher vibrational levels are absorptively pumped. The first effect can have serious consequences for line selection, since it becomes possible that certain good atmospheric transmission lines [e.g., 6 → 5, P(10)] may never be attainable from a high pressure

device. ($6 \rightarrow 5$, P(10) has never been observed from our e^--beam device even at total pressures ~85 Torr at 100°K.) The second possibility may have serious consequences for degradation of the optical extraction efficiency, gas heating, and temperature dependence of the predicted characteristics. These are discussed in the next section. Table II presents, as an example, a summary of lines which are resonant with transitions which are desirable for atmospheric transmission.

TABLE II. RESONANT TRANSITIONS FOR SELECTED CO LINES WITH GOOD ATMOSPHERIC TRANSMISSION (U)
(Unclassified)

Laser Line	Frequency (cm^{-1})	Attenuation Range (km)	Resonant Transitions	$\Delta\nu(cm^{-1})$
$6 \rightarrow 5$ P(9)	1977.264	13.3	$8 \rightarrow 7$ R(4)	.443
$6 \rightarrow 5$ P(10)	1973.285	14.3	$8 \rightarrow 7$ R(3)	-.111
			$9 \rightarrow 8$ R(11)	-.095
			$10 \rightarrow 9$ R(20)	-.018
$5 \rightarrow 4$ P(9)	2003.154	18.5	$7 \rightarrow 6$ R(4)	.101
			$8 \rightarrow 7$ R(12)	.238
$5 \rightarrow 4$ P(14)	1982.754	13.2	$4 \rightarrow 3$ P(20)	-.011
			$9 \rightarrow 8$ R(14)	.185
$5 \rightarrow 4$ P(15)	1978.575	22.7	- -	-
$5 \rightarrow 4$ P(16)	1974.362	15.4	$7 \rightarrow 6$ P(3)	-.032
$5 \rightarrow 4$ P(20)	1957.189	30.3	$6 \rightarrow 5$ P(14)	.151
			$9 \rightarrow 8$ R(6)	.145
$4 \rightarrow 3$ P(7)	2037.113	11.5	- -	-
$4 \rightarrow 3$ P(8)	2033.132	41.7	$6 \rightarrow 5$ R(5)	.313
$4 \rightarrow 3$ P(9)	2029.117	33.3	$6 \rightarrow 5$ R(4)	-.244
			$7 \rightarrow 6$ R(12)	-.311
$4 \rightarrow 3$ P(10)	2025.068	13.3	- -	-
$4 \rightarrow 3$ P(13)	2012.723	11.2	$3 \rightarrow 2$ P(19)	-.101
$4 \rightarrow 3$ P(15)	2004.326	22.7	$6 \rightarrow 5$ P(2)	.165
$4 \rightarrow 3$ P(20)	1982.765	13.0	$5 \rightarrow 4$ P(14)	.011
			$9 \rightarrow 8$ R(14)	.196
$3 \rightarrow 2$ P(5)	2071.146	40.0	$4 \rightarrow 3$ R(1)	-.250
			$6 \rightarrow 5$ R(17)	-.333
$3 \rightarrow 2$ P(8)	2059.200	10.0	$5 \rightarrow 4$ R(5)	-.035
			$6 \rightarrow 5$ R(13)	.018
$3 \rightarrow 2$ P(10)	2051.066	16.1	- -	-
$3 \rightarrow 2$ P(13)	2038.615	16.9	$2 \rightarrow 1$ P(19)	.042
			$7 \rightarrow 6$ R(15)	-.099
$3 \rightarrow 2$ P(15)	2030.148	20.8	$5 \rightarrow 4$ P(2)	-.149

*Calculations of D. K. Rice based on molecular absorption through horizontal path at sea level in a mid latitude Winter atmosphere. This model utilizes the McClatchey AFCRL major atmospheric constituent data covering wavelength from 1 μm to 20μm.

5.3 OPTICAL EXTRACTION AND EFFICIENCY

(U) Theoretical calculations of bulk, optical extraction have generally shown that quantum efficiencies seem to approach a universal steady state value of approximateiy 90%, with littie dependence on molecular temperaiure or electrical pumping rates. For exampie, the family of curves in Figure 1 show littie sensitivity to the (scaled) pump rate W_e/P_{CO}^2, and similar curves are predicted at high temperature, suggesting that there is a negligibie dependence on temperature. It is found experimentally, however, that room temperature operation is significantly less optimistic than that predicted by existing theoreticai models, and quantum efficiencies of ~90% have not yet been attained even at low temperature. Degradation of opticai extraction efficiency, as well as the poor agreement with high temperature predictions, can both be qualitativeiy explained by the resonant absorption hypothesis. The optical extraction per unit volume is determined by a combination of quantum efficiency and output coupiing efficiency, where the latter is the ratio of the output coupiing loss/pass, divided by the totai optical loss/pass. If a line has attained sufficient gain to lase, absorption in the medium is effectively added to other losses (e.g. windows) in the cavity, and thus, absorption in the medium (which is typically in higher v-bands) will resuit in a degraded coupling ratio. Furthermore, the absorptive pumping of higher vibrationai levels wiil degrade the predicted quantum efficiency, since VV heating wiil be increased and the capacity to extract energy in the form of iaser radiation is reduced.

5.4 TEMPERATURE DEPENDENCE

(U) At higher temperatures, for a given density the collision broadened half-width is increased, and therefore the number of resonant absorption processes that may contribute is increased. Furthermore, the P(J) transitions are shifted to higher J values, which may result in R(J) resonances with more severe absorptive characteristics. Lastly, gain and absorption are strong functions of temperature, and although the oscillator operatec with saturated gain equal to loss, the increased absorptive pumping of higher vibrational ievels may explain the poor performance characteristics of high pressure room temperature devices. It has often been speculated that the unexpiained discrepancy in temperature dependence may be due to inadequate knowledge of the VV cross-relaxation rates. However, it can be shown by a simple argument that, if the functional dependence of the VV rates on the ievels v is held fixed, adjusting the magnitude of the VV rate constant cannot account for the insensitivity that the quantum efficiency shows to temperature. To see this, suppose that the famiiy of curves shown in Figure 1 corresponded to $T = 300^{\circ}K$; then, for fixed excitation W_e, the effect of changing the VV rate can be determined by examining curves for different vaiues of W_e/p_{CO}^2, since that parameter is merely a measure of the eiectricai pumping per molecule relative to the rate of VV cross relaxation. Since the family of curves in Figure 1 span more than two orders of magnitude for the parameter W_e/p_{CO}^2, it is not likely that better agreement between theory and experiment wiil be attainable by adjusting the VV rates with only a multiplicative constant. Other possibilities, for explanation of the anomolous temperature dependence are that the structure of the VV rate matrix is drastically different, or that VT processes from high vibration ievels are much faster than predicted from extrapolation of SSH

theory (fit to 1→0 experimental data), which is not likely. Resonant self absorption may, therefore, resolve the unexplained sensitivity to temperature dependence.

5.5 FREQUENCY PULLING AND PUSHING

(U) Because the gains for all of the CO transitions are now sums of Lorentzians for all of the resonant lines, the frequency dependence of the gain is distorted. It is, therefore, possible that one of the important consequences of self-absorption may be the shifting of the oscillation frequency from the line center. Figure 10 illustrates a case for a line with gain centered at frequency υ_o, with a neighboring absorbing line located at $(\upsilon_o + \Delta\upsilon)$, where $\Delta\upsilon$ is the collision broadened half-width. The net gain, as a function of frequency, is a sum of these two Lorentzians and is also shown. The line center for the net gain occurs at a frequency shifted away from υ_o (in this case pushed) by an amount $\delta\upsilon$. Similar effects resulting in pulling can result if the neighboring resonant line exhibits gain rather than absorption. The magnitude of these frequency shifts may be important for atmospheric transmission. If they are important (e.g. $>.02\ cm^{-1}$) the effect will not be detected by experimental absorption measurements based on low pressure CO laser probes oscillating on transition line centers.

6. REFERENCES

1. M. M. Mann, D. K. Rice and R. G. Eguchi, "An Experimental Investigation of High Energy CO Lasers," Paper B.7 presented at the VIII International Quantum Electronics Conference, June 10-13, 1974, San Francisco, California.
2. R. E. Center, "High-Pressure Electrical CO Laser," IEEE J. Quant. Elect. QE-10, 208 (1974).
3. W. B. Lacina and B. B. O'Brien, Jr., "Electron Beam Stabilized CW Electric Discharge Laser in Supersonically Cooled CO Gas Mixtures - Part II - Projected Large Scale System," presented at The First Classified Conference on High Energy Laser Technology, San Diego, California, October 1974.
4. W. B. Lacina, "Kinetic Model and Theoretical Calculations for Steady State Analysis of an Electrically Excited CO Laser Amplifier System," Northrop Rpt NCL 71-32R, August 1971.
5. W. B. Lacina, M. M. Mann, and G. L. McAllister, "Transient Oscillator Analysis of a High Pressure Electrically Excited CO Laser," J. Quant. Elect. QE-9, 588 (1973).
6. W. Q. Jeffers and C. E. Wiswall, "Analysis of Pulsed CO Lasers," J. Appl. Phys. 42, 5059 (1971).
7. R. E. Center and G. E. Caledonia, "Theoretical Description of the Electrical CO Laser," Appl. Phys. Lett. 19, 211 (1971). "Vibrational Distribution Functions in Anharmonic Oscillators," J. Chem. Phys. 55, 552 (1971).
8. J. W. Rich, "Kinetic Modeling of the High Power Carbon Monoxide Laser," J. Appl. Phys. 42, 2719 (1971).
9. R. L. McKenzie, "Vibrational Relaxation and Radiative Gain in Expanding Flows of Anharmonic Oscillators," NASA Tech. Note, NASA TN D-7050, March 1971.
10. S. D. Rockwood, J. E. Brau, W. A. Proctor, and G. H. Canavan, "Time-Dependent Calculations of Carbon Monoxide Laser Kinetics," IEEE J. Quant. Elect. QE-9, 120 (1973).
11. W. B. Lacina, "Scaling Generalizations for a Pulsed CO EDL," Northrop Rpt NRTC 73-43R, October 1973.
12. F. E. C. Culick, P. I. Shen, and W. S. Griffin, "Studies of the Acoustic Waves Formed in an Electrical Discharge CO Laser Cavity," presented at AIAA ASME Thermophysics and Heat Transfer Conference, Boston, Massachusetts, July 15-17, 1974.

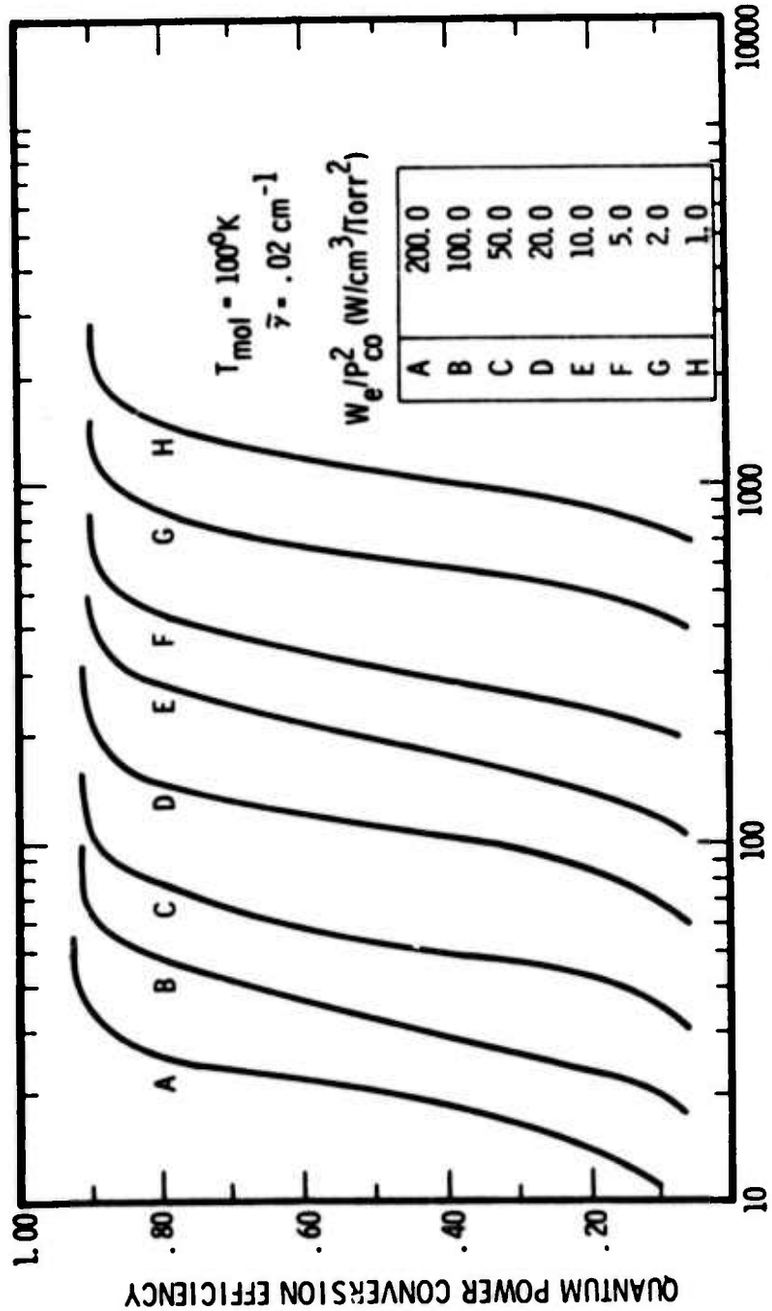

FIGURE 1. QUANTUM POWER CONVERSION EFFICIENCY AS A FUNCTION OF SCALE TIME $P_{CO}t$, FOR SEVERAL VALUES OF SCALED EXCITATION POWER W_e/P_{CO}^2, AT 100°K. (U)

(Unclassified figure)

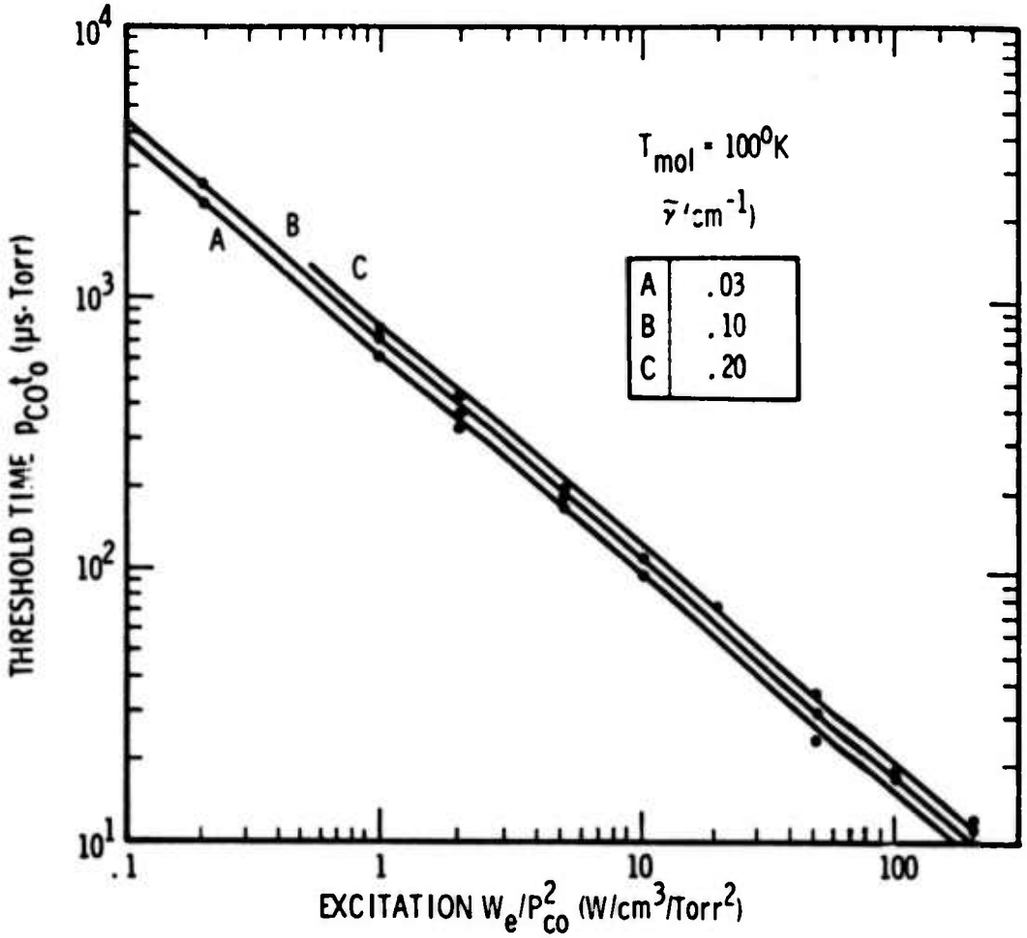

FIGURE 2. SCALED THRESHOLD TIME $p_{CO}t_o$ AS A FUNCTION OF SCALED EXCITATION W_e/p_{CO}^2 FOR SEVERAL VALUES OF LOSS $\bar{\gamma}$ AT 100°K. (U)

(Unclassified figure)

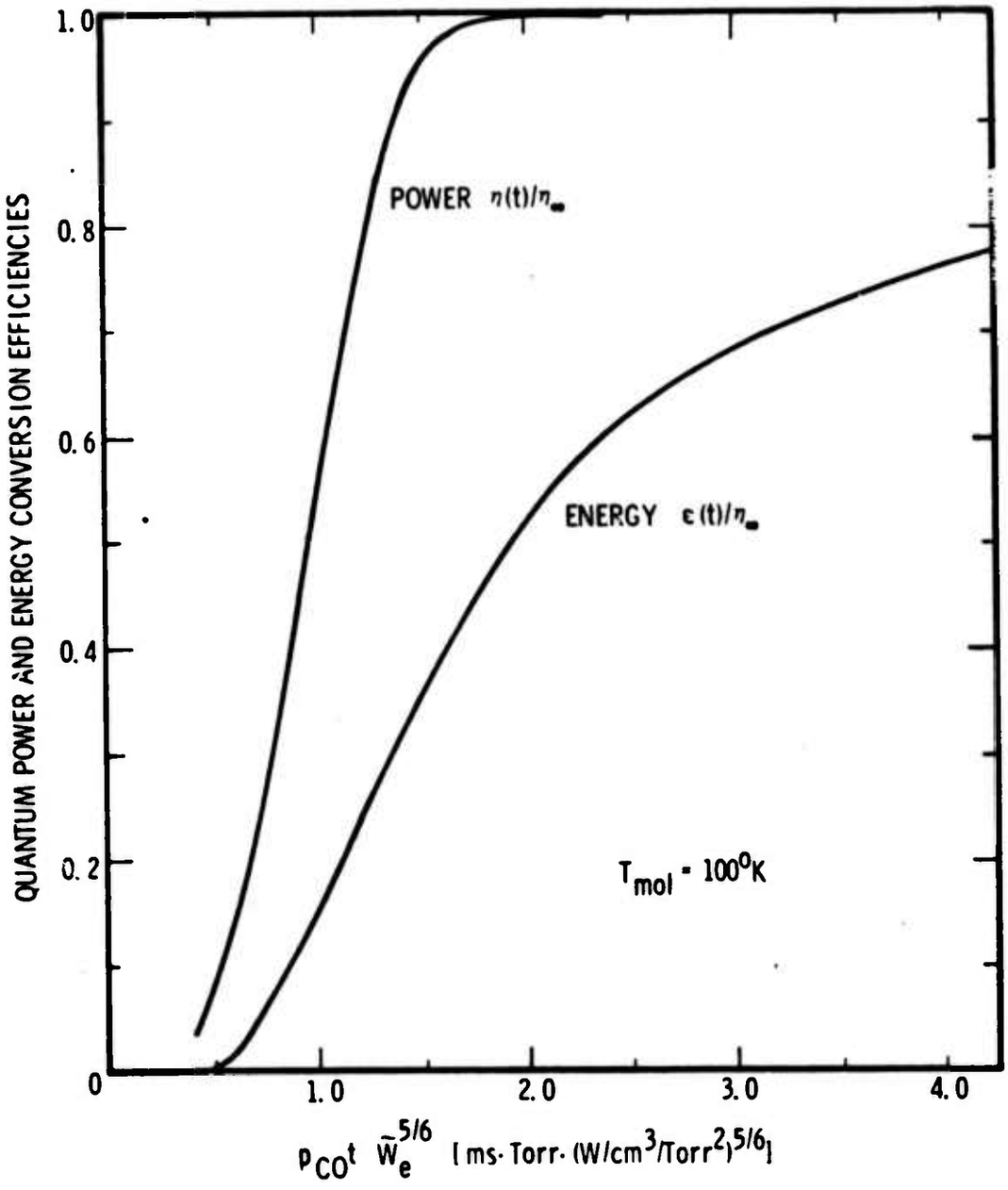

FIGURE 3. GENERALIZED POWER AND ENERGY CONVERSION EFFICIENCIES AS A FUNCTION OF $p_{CO}t(W_e/p_{CO}^2)^{5/6}$ AT 100°K. (Note that, without the 5/6 exponent, the units of the horizontal axis would correspond to energy deposition in J/ℓ/Torr(CO)). (U)

(Unclassified figure)

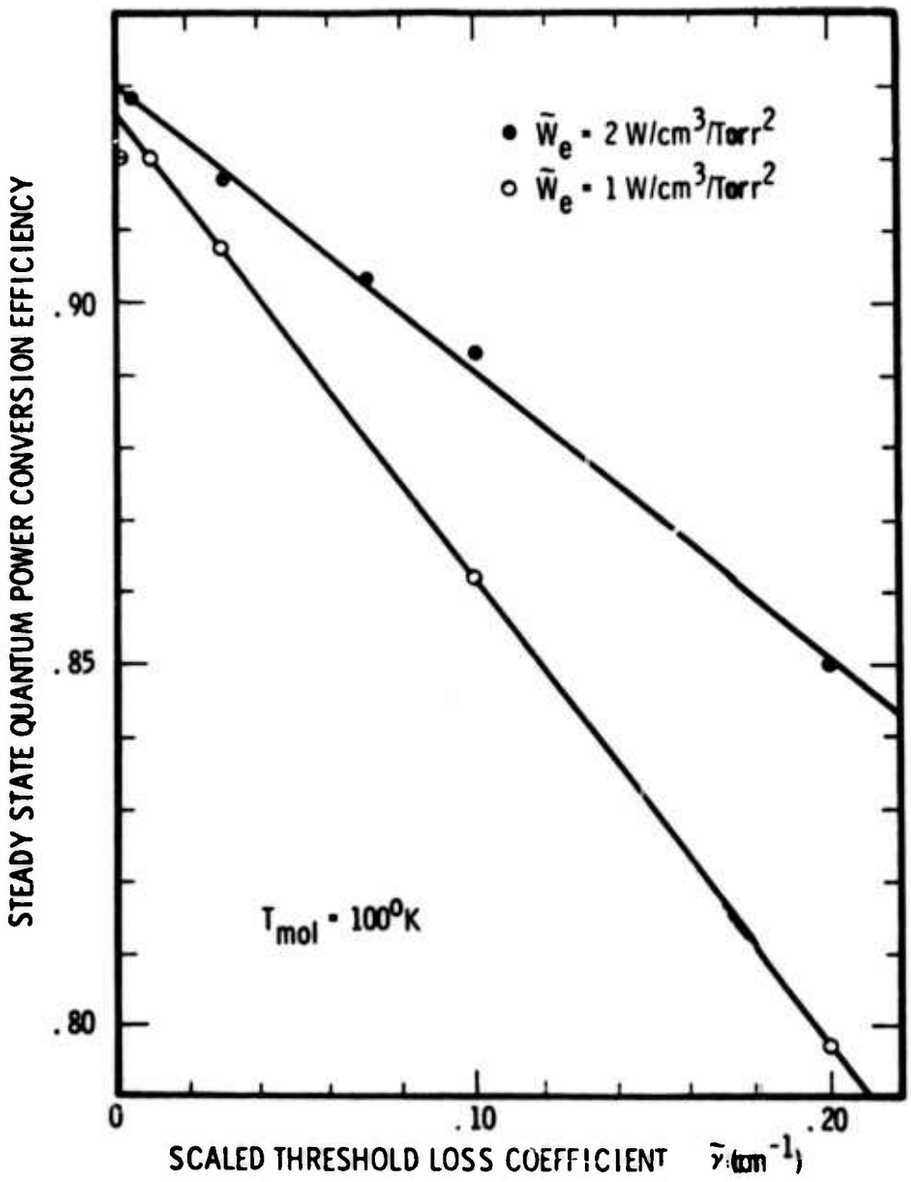

FIGURE 4. STEADY STATE POWER EFFICIENCY AS A FUNCTION OF SCALED THRESHOLD LOSS COEFFICIENT $\bar{\gamma}$ FOR AN OSCILLATOR, FOR TWO VALUES OF SCALED EXCITATION $\bar{W}_e = W_e/p_{CO}^2$. Note that the slopes of these curves are proportional to $\bar{I}_s/\bar{W}_e$ where $\bar{I}_s$ is the scaled saturation intensity. (U)

(Unclassified figure)

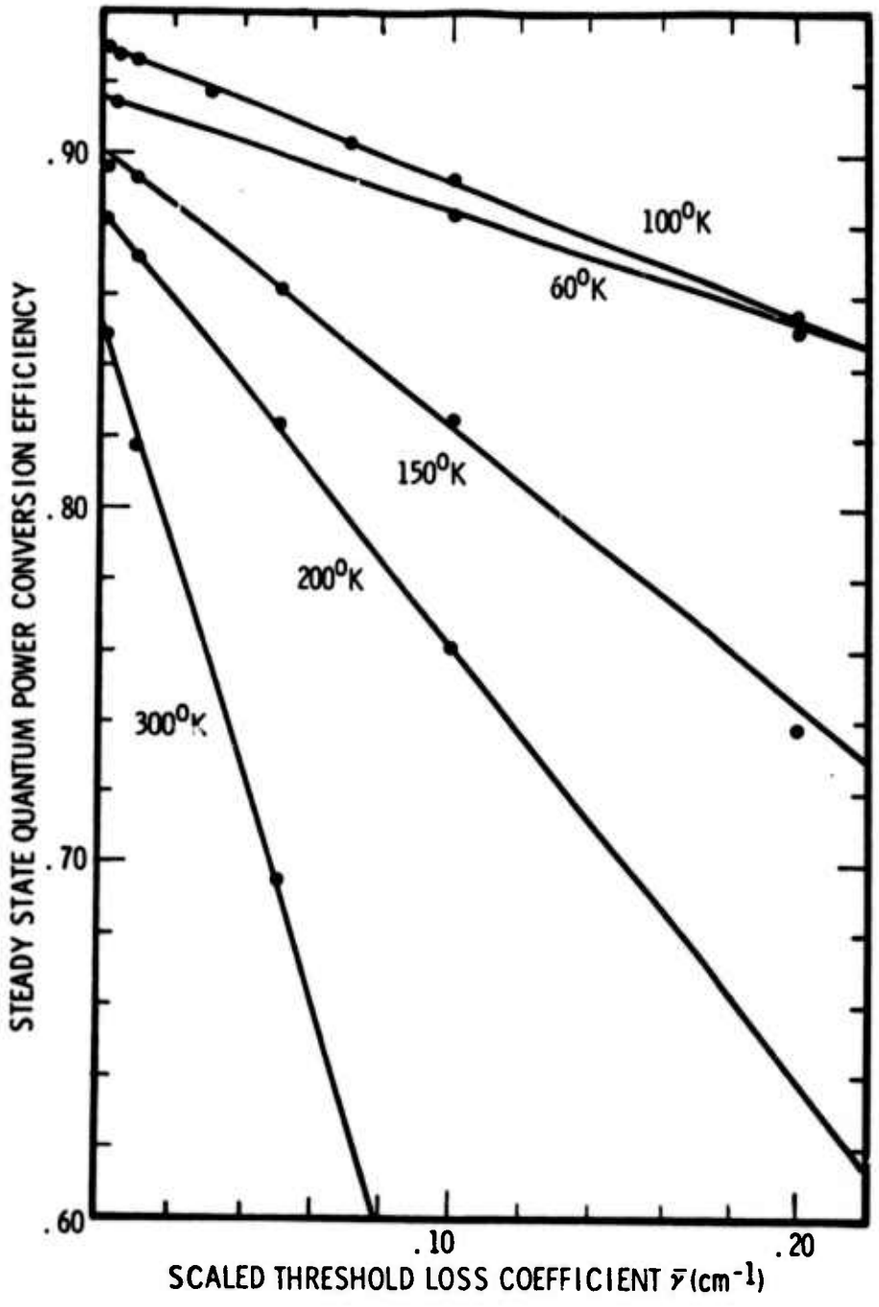

FIGURE 5. STEADY STATE POWER EFFICIENCY AS A FUNCTION OF SCALED THRESHOLD LOSS COEFFICIENT $\bar{\gamma}$ FOR SEVERAL DIFFERENT TEMPERATURES, FOR $\tilde{W}_e$ = 2 W/cm^3/TORR(CO)^2. (U)

(Unclassified figure)

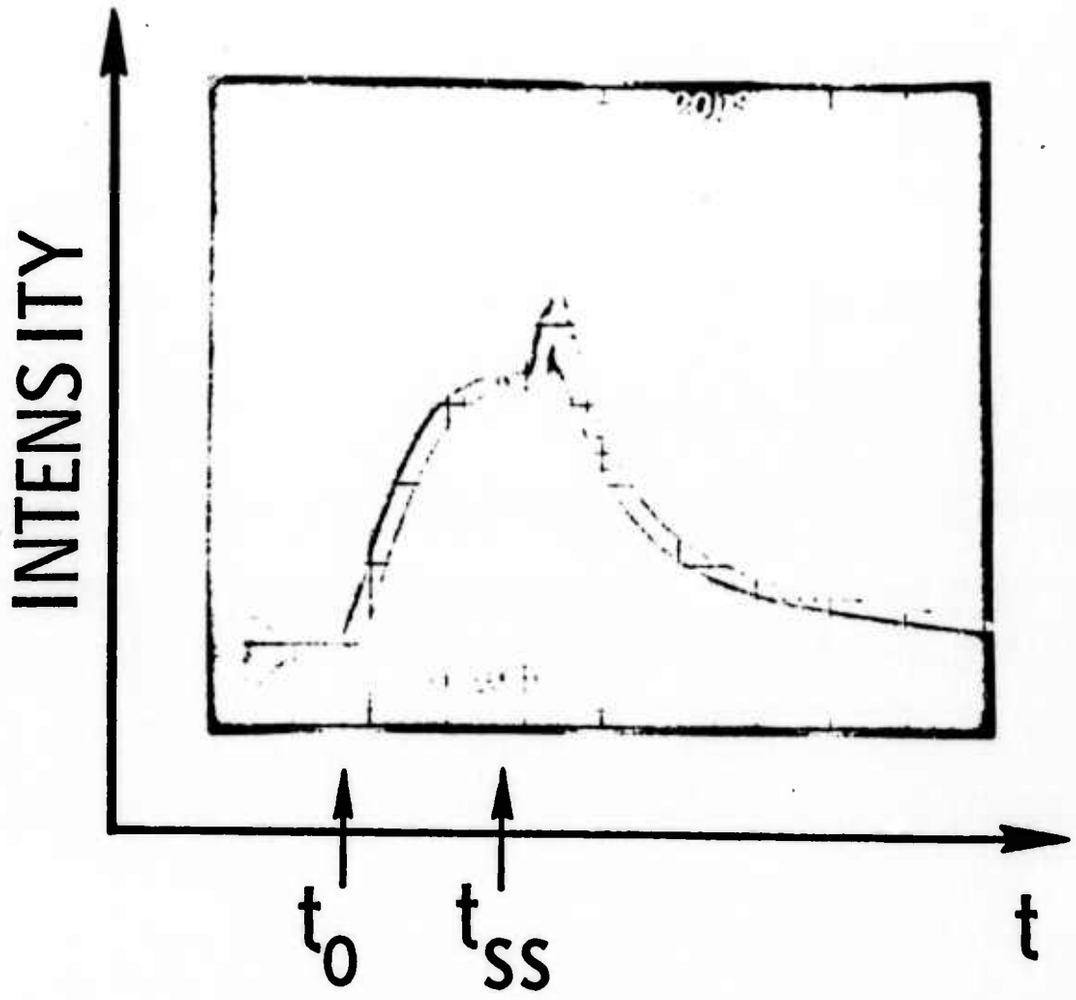

FIGURE 6. SCOPE TRACE OF TOTAL OPTICAL OUTPUT POWER AS A FUNCTION OF TIME FOR A TYPICAL e^--BEAM LASER PULSE. (U)

(Unclassified figure)

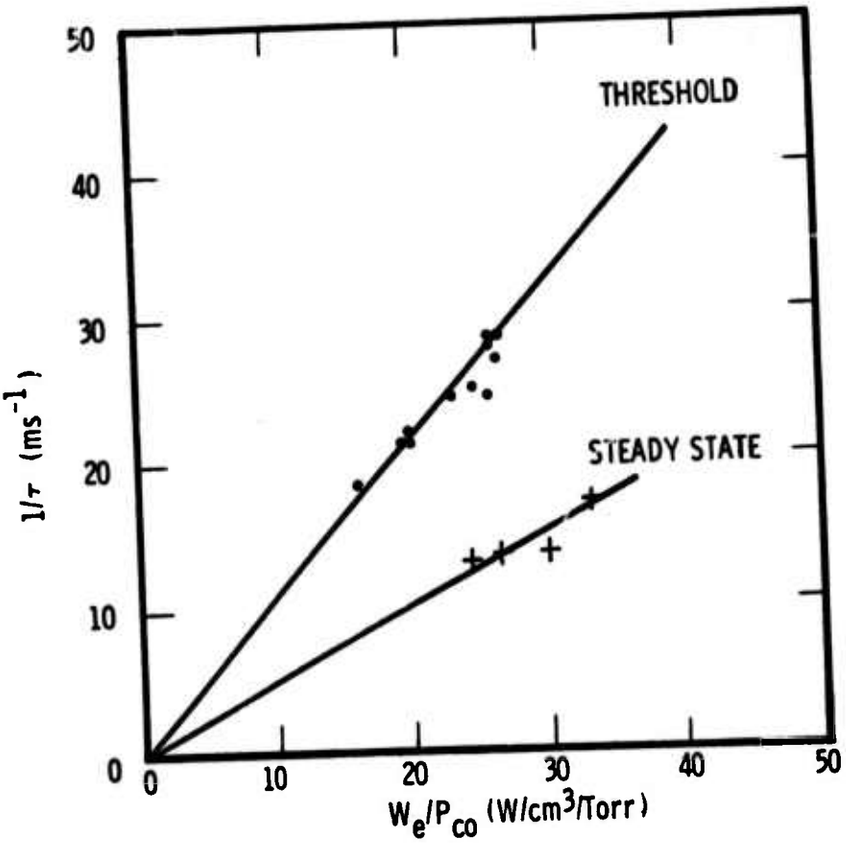

FIGURE 7. INVERSE OF EXPERIMENTALLY OBSERVED TIMES REQUIRED FOR ATTAINMENT OF THRESHOLD AND STEADY STATE FOR A CO/Ar GAS MIXTURE, AS A FUNCTION OF W_e/P_{CO}. (U)

(Unclassified figure)

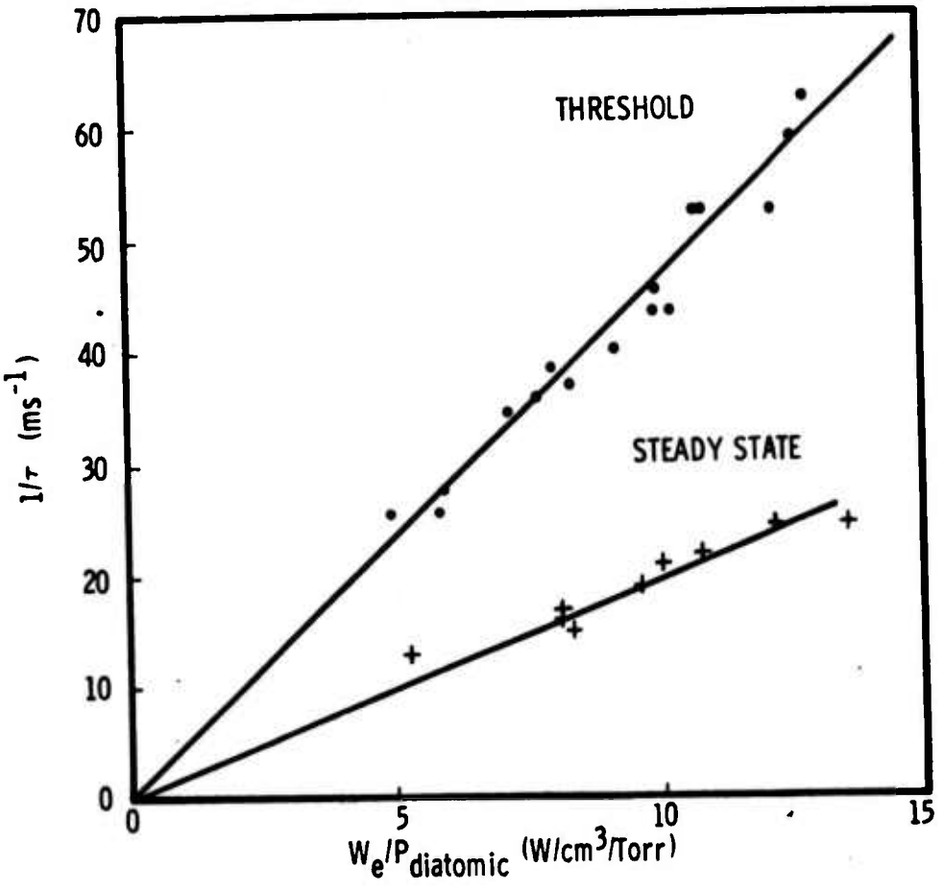

FIGURE 8. INVERSE OF EXPERIMENTALLY OBSERVED TIMES REQUIRED FOR ATTAINMENT OF THRESHOLD AND STEADY STATE FOR A 1:6 CO/N_2 GAS MIXTURE. (U)

(Unclassified figure)

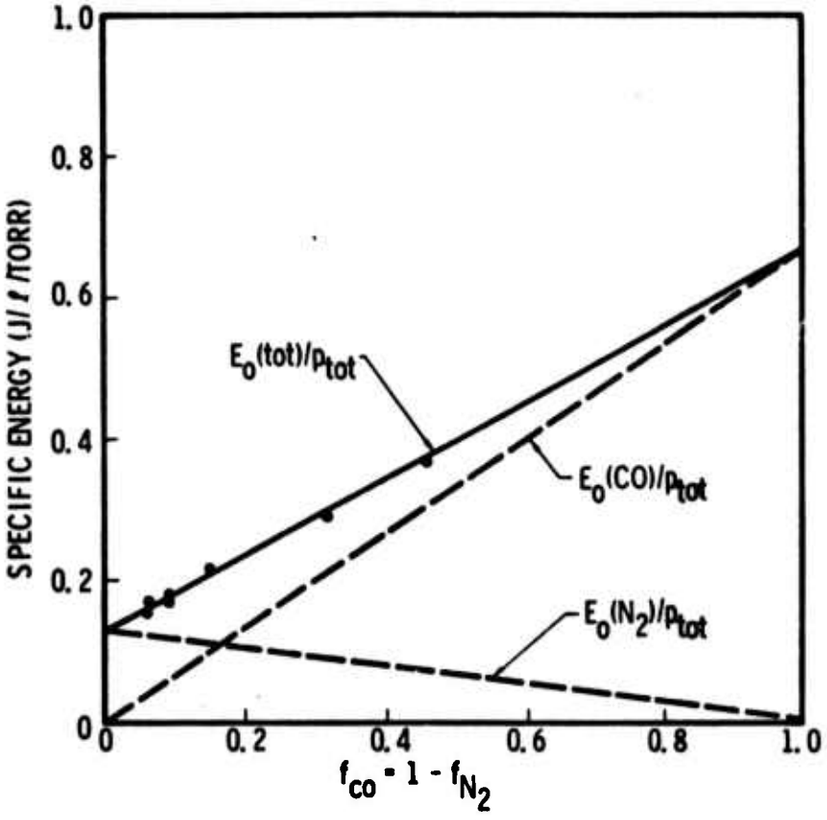

FIGURE 9. EXPERIMENTAL SPECIFIC ENERGIES AS A FUNCTION OF FRACTIONAL CO CONTENT REQUIRED FOR ATTAINMENT OF LASER THRESHOLD FOR CO/N_2 GAS MIXTURES. (U)

(Unclassified figure)

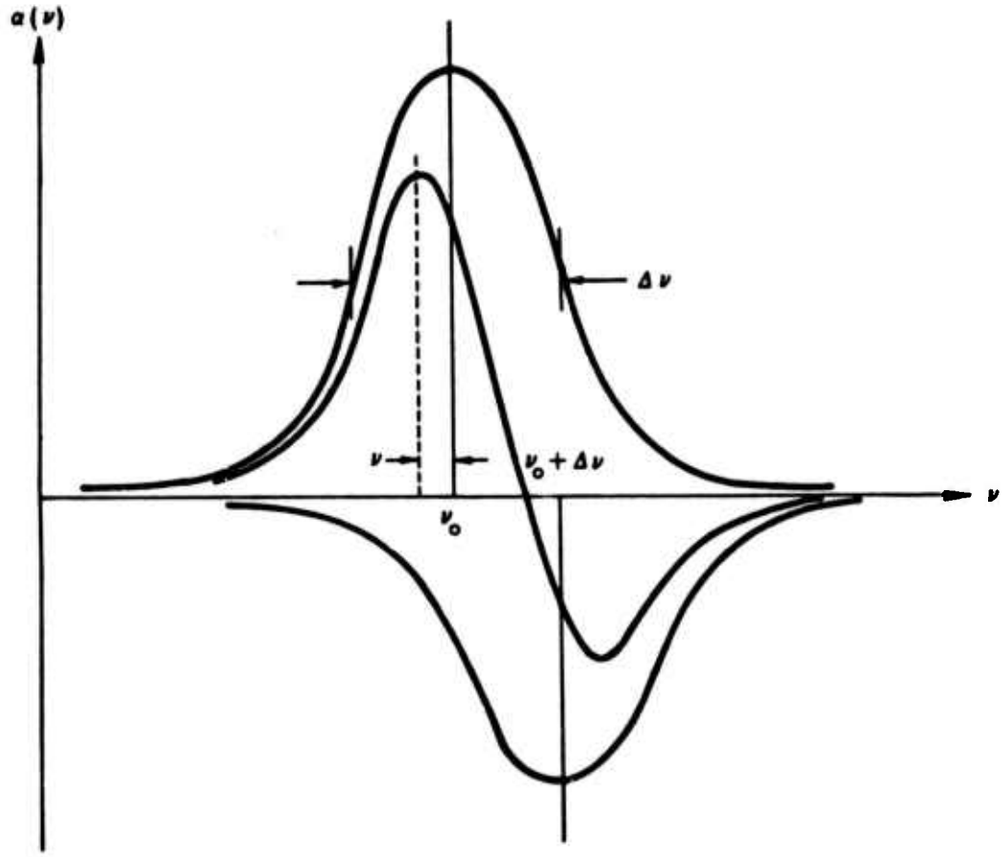

FIGURE 10. FREQUENCY DEPENDENT GAIN FOR OVERLAPPING COLLISIONALLY BROADENED NEAR RESONANT TRANSITIONS. (U)

(Unclassified figure)